The work reported in this document was performed at Lincoln Laboratory,

This technical report has been reviewed and is approved for publication.

FOR THE COMMANDER

Raymond L. Loiselle

Raymond L. Loiselle, Lt. Col., USAF
Chief, ESD Lincoln Laboratory Project Office

MASSACHUSETTS INSTITUTE OF TECHNOLOGY

LINCOLN LABORATORY

DISTRIBUTED SENSOR NETWORKS

SEMIANNUAL TECHNICAL SUMMARY REPORT
TO THE
DEFENSE ADVANCED RESEARCH PROJECTS AGENCY

1 JANUARY – 30 SEPTEMBER 1977

ISSUED 6 JANUARY 1978

LEXINGTON   MASSACHUSETTS

ABSTRACT

Progress on the selection of a Distributed Sensor Networks program application problem, discussion of system elements, formulation and testing of multisite detection and location algorithms, and review of the fundamentals of sensitivity analysis are reported. Design and execution of an acoustic/seismic field experiment, and analysis and evaluation of experimental data including preliminary determination of acoustic detection ranges, spectral signatures, and direction determination capabilities are also described.

CONTENTS

GROUP 22

CONTRIBUTORS
TO
DISTRIBUTED SENSOR NETWORK PROGRAM

Lacoss, R. T.
Landers, T. E.

I. INTRODUCTION AND SUMMARY

This is the first Semiannual Technical Summary report of the Lincoln Laboratory Distributed Sensor Networks (DSN) program. Our program is part of an ARPA-sponsored program with participation by several contractors. The overall program is ultimately aimed at identifying and demonstrating innovative applications of new developments in computer network theory and computer science to systems employing multiple sensors for target surveillance and tracking. Such systems are made up of sensors, data bases, and processors distributed throughout an area, interconnected by an appropriate communication system, and serving users who are also distributed and served by the same communication system. A major hypothesis to be verified is that through suitable netting and distributed processing the information from individual sensors of limited capacity and/or range can be combined to yield an effective survivable surveillance system at a feasible cost.

The DSN program is currently in a feasibility and planning phase which will be completed in FY 78. We expect that the present research effort will verify that a suitable test bed can be created within which it will be possible to develop and demonstrate DSN concepts and technology. The Lincoln program concentrates upon overall system questions involving sensor options, basic single-sensor and multisite processing algorithms, system trade-offs, networking, data flow, development of workable DSN system concepts, and the development of a test-bed plan.

The major accomplishments of this first reporting period are summarized below.

A. DSN System Issues

The following summarizes our accomplishments relating to four distinct system problem areas.

First, a number of possible DSN applications were reviewed. From these we have identified the surveillance of low-flying aircraft, using a combination of acoustic, seismic, and/or simple radar sensors, as a problem for which such a test bed might be developed. The low flying aircraft problem serves to focus the system issues, but the effort is aimed at results which are general enough so that they can be adapted to a number of scenarios and sensor options.

Second, a general structure and major functional elements of a DSN have been tentatively identified. This furnishes a basis for interaction with other program participants and for factoring out DSN subproblems.

Third, a study, using simulation, has been completed for one major subproblem. This subproblem is the initial integration of multiple sensor reports to declare the possible existence of new targets and generate initial location estimates. It is assumed that individual sensors do detect targets but that they do not sufficiently localize the target and may report too many false detections. A PDP-11 computer study of the interaction of such reports for range-only sensors has been completed. The simulated sensor reports included range measurements and false alarms. An elementary multisite detection algorithm was programmed and applied to the simulated data. Through demonstration in a simple case, this study verified that proper use of data redundancy should allow a DSN to accommodate a reasonable number of single-sensor false alarms and to control ghosting in the presence of multiple targets. The difficulty of generalizing our specific multisite detection algorithms to more complicated situations has suggested a

1

different approach to be investigated. The new approach will be based upon a directed search of target state space and is a decision theoretic approach.

Fourth, a simple statistical model for the multisite location problem has been selected so that location performance can be evaluated in terms of error ellipsoids whose size and shape depend upon the kinds of measurements made, measurement errors, and target-sensor geometry. The basic formulation for such a sensitivity analysis has been completed. This will be the foundation for actual multisite location sensitivity studies. It will also be used to provide sensitivity information needed for the future design of improved multisite detection algorithms.

B. Sensor Investigation

Our investigation of sensor issues has thus far concentrated upon acoustic and seismic sensors. Available data and reports in the literature indicated the potential utility of acoustic sensors. However, the basic capability of such sensors for detecting, tracking, and identifying aircraft was unknown so that we felt it important to investigate this class of sensors in detail early in our work.

A controlled experiment was designed and executed to provide acoustic and seismic array data for low-flying aircraft. These data were to enable us to evaluate the detection, tracking, and identification capabilities of such sensors. Precise target location and atmospheric propagation characteristics were integral elements of the field experiment.

A preliminary analysis of some of the experimental data has been completed. This work included visual reduction of analog field recordings to estimate detection range, spectral analysis of digitized data to find tracking and identification characteristics, coherent array processing to establish direction measurement capability, and analysis of meteorological data to determine the effects of atmospheric propagation phenomena. The initial results indicate that acoustic sensors can provide reliable accurate tracking, identification, and location data for ranges of at least several to ten or more kilometers.

2

II. DSN SYSTEM ISSUES

A. Application Selection

Several surveillance problems to which DSN concepts might be applied have been reviewed. Our purpose has been to select a problem which will help to focus the DSN effort and for which a test bed might eventually be developed. Possible application areas we considered included general tactical information systems using a broad range of surveillance data types, surveillance of low-flying aircraft, and underwater surveillance systems.

The surveillance of low-flying aircraft has been selected as the application which will initially be used to focus our DSN efforts. An informal working paper discussing three variations of the low flying aircraft problem has been prepared for discussions with other program participants. The working paper also discusses the problem of passive acoustic underwater surveillance.

The low flying aircraft surveillance system of particular interest to us is one which will accomplish area surveillance using ground-based acoustic/seismic sensors and/or very inexpensive radars. Such a system can be an effective gap filler operating in conjunction with more traditional radar systems. It might be the only practical way to maintain adequate surveillance of some areas without continuous airborne radar platforms. In addition to its validity as a system concept for low flying aircraft surveillance, such a system seems to be a practical one in terms of eventually developing a test bed of modest size and cost.

B. System Structure

We have begun to define the elements of a DSN and to formulate some basic system concepts. We have kept the low flying aircraft problem in mind to be sure that our ideas make sense in a specific context. Our current breakdown of a DSN into ten major elements and functions is summarized below, followed by a brief discussion of a proposed DSN structure which can serve as a strawman structure for future consideration.

Sensors:– Sensors receive signals from targets. They may respond to signals normally radiated by the target or may respond to signals which result from illumination of the target.

Illuminators:– In an active DSN, certain sites radiate energy which can interact with targets to produce signals received by sensors. Illuminators need not be colocated with sensors, and the relationship between illuminators and sensors need not be one to one.

Front-End Processing:– In a DSN, the raw detector data will be processed at the sensor site to perform initial target detections, extract parameters of interest (for location and target identification), and thus allow for a reduced data flow away from the site. The front end is the first level of processing in a DSN.

Data Base Management:– One can think of a DSN as a system whose primary function is to operate on the distributed time-varying data base generated by the front end to produce more directly useful target data bases. The design, control, and management of these data bases is a critical system function.

Multisite Detection and Location:– Multisite detection, discussed at some length in a later section, is the next level of target data processing above front-end processing. The function is to combine previously unassimilated multisite data to detect and assign initial locations and

identities to possible new targets. It is important to have a low false dismissal while avoiding high false alarm rates and excessive numbers of ghosts.

Tracking:– Tracking is the processing level above multisite detection. The task is to assimilate new data associated with a target, update estimates of target parameters, and further prune possible false alarms or ghosts. The front-end processing, data management, multisite detection and tracking functions are closely interrelated.

Intersite Communication:– Communication is required to support the DSN operation. A Packet Radio Network is one option available for intersite communication. An important DSN issue will be the effect of communication system characteristics on DSN design and performance.

Sensor/Illuminator Location:– The location of sensors and illuminators must be known. These would be fixed in a permanent surveyed installation, but may require a separate subsystem for deployable DSNs. For a deployable system, a modified packet radio may be adapted to provide the needed sensor location information.

Coordination and Control:– The distributed realization of functions (e.g., illuminator scheduling, front-end processing, data base management, multisite detection and tracking) must be coordinated and controlled.

User Services:– The main purpose of a DSN is to supply information to users of the system. User services interface to track files and other information distributed throughout the DSN. The present concept is that user services access data but do not modify the basic data or the functioning of other elements which produce the data bases. However, user services may take advantage of spare processor capacity at any level to augment data bases for their own purposes.

Figure II-1 depicts our present ideas about an appropriate DSN system organization and suggests the context for our multisite detection research effort. The system structure consists of two overlaid grids of two different densities. The sensor (and colocated front-end processing and data storage) grid is most dense. The less dense grid is a grid of processors responsible for multisite detection. A similar structure might also apply for tracking and higher level user services, but we exclude a discussion of these issues here for simplicity. Our concept allows the multisite detection processor grid to be as dense as the sensor grid, but we expect engineering considerations to mitigate toward a more dense sensor grid.

The overall surveillance area is divided into regions of primary responsibility for the multisite detection processors. These areas can be fixed by simple common algorithms or may be more actively negotiated. The responsibility for any point in surveillance space is assigned to a specific processor. Boundary areas between areas of responsibility are potential problem areas. These areas result from the fact that the area in which a processor can locate targets using its assigned sensors is normally larger than its area of prime responsibility and also that its locations may be very approximate. The overlap areas are critical and coordination of multisite detection (as well as tracking and other functions) for those areas is an important system issue. A few other properties of the proposed structure are worthy of note. A processor can use sensors inside and outside of its area of responsibility. The same sensor (and front-end processor) may service more than one processor. The system will need to accommodate such assignments and the privileges of the different processors with respect to the sensors.
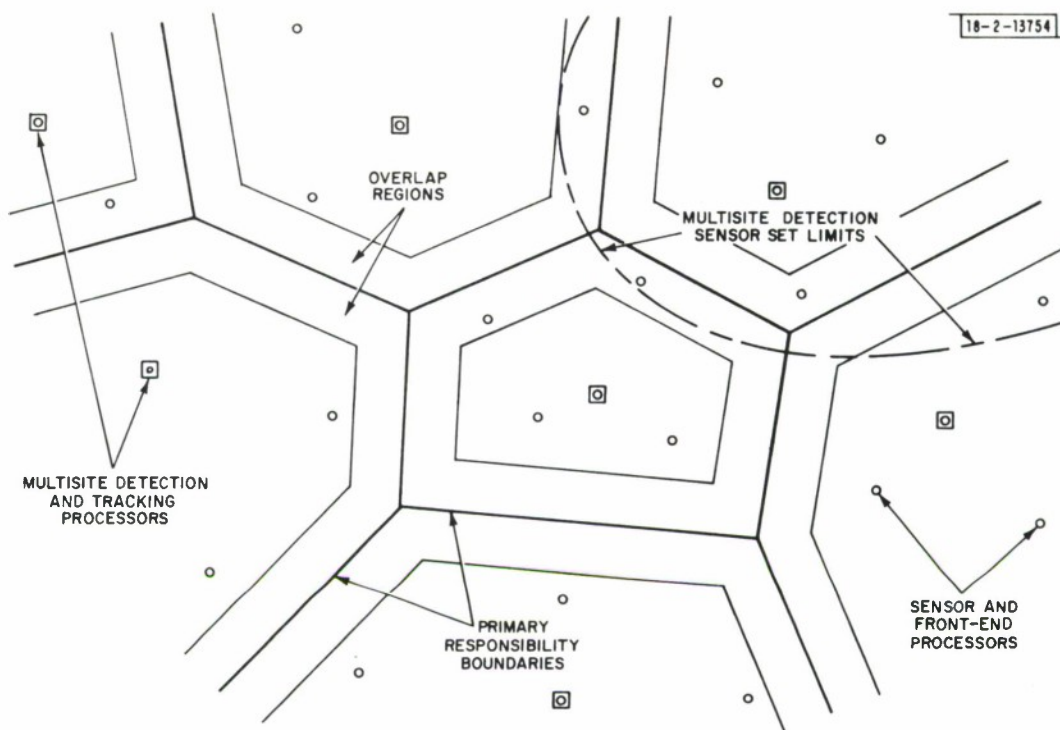
Fig. II-1.   A DSN general system structure.

C.   Multisite Detection and Location

Multisite detection is the combining of reports (detections and measured target parameters) from several sensors to obtain an initial multisite confirmation and preliminary location for targets.   In the general DSN context, we assume that a sensor cannot individually give target location and may have many false alarms so that multisite detection is essential to get tentative locations and to reject false alarms.   For example, a DSN composed of many elementary radars which individually detect and report range but give no other target information would require that the multisite detection and location function be carried out.   We selected such a system for initial study and modeling.   Results are summarized below along with a discussion of how this work has influenced our approach to multisite processing.

Our work has centered upon the possible ghosting problem in a DSN composed of simple sensors.   Ghosting is a classical radar system problem.   Ghosts are apparent targets which are consistent with data but which do not correspond to real targets.   This situation can occur when there are multiple targets in the area or when sensors generate false alarms.   Our present approach to deghosting is predicated on the hypothesis that ghosting can be minimized or eliminated if there is redundant data.   The technique is to maximize the amount of data explained by targets while at the same time minimizing the number of targets needed to explain the data.   This is a general idea which is not limited to range-only systems.   However, our simulation was specific and an attempt to expand to other kinds of sensors caused us to modify our approach as is discussed below.

1. Software

A computer simulation of the multisite detection and location function of a DSN operating with range-only sensors and any number of targets has been written. The code is written in the C language and runs on a PDP-11 under the UNIX operating system. The program treats each instant of time independently. At each instant, one routine generates range reports which are then processed by another routine which tries to reconstruct the target positions from those reports.

The range report generation code creates reports based upon the target-sensor geometry and several parameters controlling sensor performance. These parameters are (a) R_{max}, the nominal maximum sensor range; (b) σ, the standard deviation of errors in measured range; (c) n_{fa}, the number of false range reports generated by the sensor at each reporting period; and (d) the range interval (r_{min}, r_{max}) over which false alarms can occur. For each sensor, the program generates n_{fa} false range reports in the (r_{min}, r_{max}) interval using a pseudorandom number generator. In addition, a range report is generated for all targets within the maximum sensor range. For each target, the true range plus a random error constitutes the report. The error is another pseudorandom number with zero mean and standard deviation σ.

The separate target reconstruction routine (multisite detection and location algorithm) checks all possible combinations of range reports three at a time to locate possible targets. In the case of M sensors each reporting K ranges, this involves checking $M!K^3/[(M-3)!3!]$ triplets of observations. A list of possible targets is constructed by the program as targets are found. Redundant entries in the list are removed and noted as discussed below.

We can also require that more than three range measurements correspond to a target before a multisite detection is declared. In this case, a three-report detection is accepted as a preliminary multisite detection and a search of the remaining reports is made to find additional corroborating data before a final multisite detection is declared and entered into the target list. This secondary search uses a window parameter ϵ. Given a possible target, the range to a sensor is calculated. If that range is within ϵ of one of the reports from the sensor, then the sensor is counted as corroborating the target. Any number of additional corroborations can be required.

As noted above, while the possible target list is being constructed, different sets of range reports can yield the same apparent target. This is exactly true if range reports are perfect and we use infinite precision arithmetic. However, with measurement errors and finite word sizes, one obtains a cloud of locations for a target rather than a single point. We do not save all members of this cloud but replace it with a single average point and a count of the number of members in the cloud. The condensing of the cloud is done recursively as new possible targets are generated. Any new trial target location is compared to the list, and entries which match to within the window parameter ϵ are marked. The counts of marked entries are incremented by one, and the locations are replaced by a suitable weighted average of the old value and the new matching value.

2. Experimental Results

Figure II-2 summarizes two sensor-target configurations which we have used to obtain experience with the multisite detection problem and to demonstrate the performance of algorithms. Results are given below for the cases of no targets, one target, and two targets. In all situations, the maximum radar range, R_{max}, is 6 km so for the geometries shown when a target is present
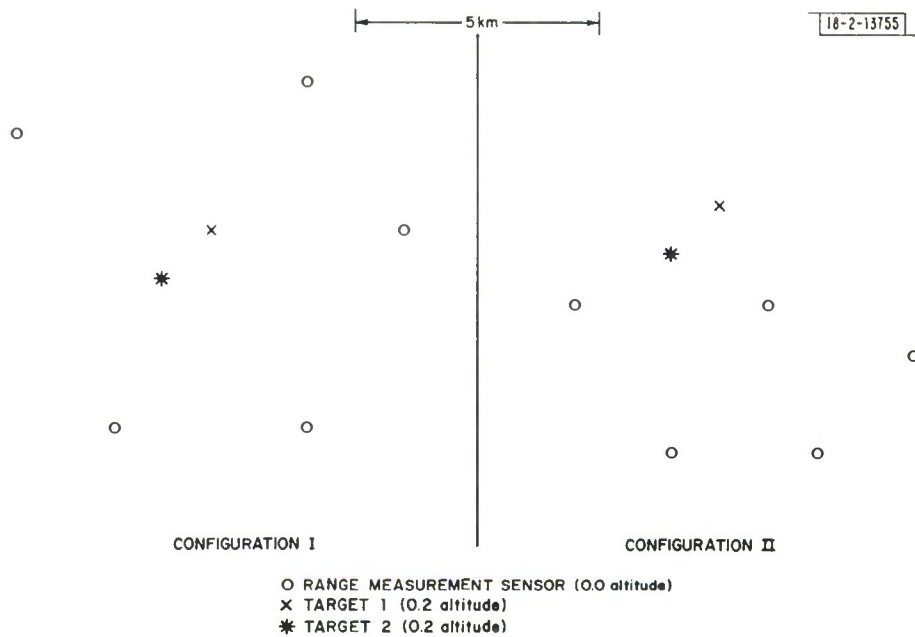
6

Fig. II-2. Sensor and target configurations for computer experiments.

it is within range of all five sensors. The single-sensor false-alarm interval (r_{min}, r_{max}) is (1, 6) in all cases. In all examples, ten runs were made using different random numbers for measurement errors and false alarms. The tabulated data represent average performance over the ten runs.

A number of runs were made with no targets in the area but with different numbers of false alarms per sensor and different values of the window parameter, ϵ. The results are summarized in Table I. As expected, the number of false multisite detections increases as ϵ decreases. This is because ϵ is essentially a clustering parameter. For small values of ϵ, a new possible target may form the nucleus of a new cluster rather than being incorporated into an already existing one. Small ϵ means more clusters with fewer points per cluster. In the limit, each cluster can contain a single point.

There is a rather large increase in the number of multisite false targets for only a modest increase in the number of false alarms at each site. The single-site false report rate will be an important DSN system parameter. It has only a linear influence upon the basic intersite data communication, but can very greatly influence the computation load and difficulty of the multisite false alarm problem.

Lastly, for this no-target experiment we note that requiring four sensors rather than three substantially reduces the number of multisite false targets. This is a manifestation of the general principle that false targets can be rejected if true targets can be assumed to be supported by sufficiently redundant data.

A number of runs have been made with a single target and two single-sensor false alarms from every site. Table II is a summary of the results. The results are given for three values of the standard deviation, σ, of range measurement errors. The same single-sensor false alarms were used for all three σ values. Also the range measurement errors for the three σ cases are just scaled versions of a single set of range report errors.

7

TABLE I

AVERAGE NUMBER OF FALSE TARGETS DECLARED AS A FUNCTION OF THE CLOSENESS PARAMETER, ϵ, AND THE NUMBER OF FALSE ALARMS PER SENSOR, n_{fa}. RESULTS SHOWN FOR TWO FIVE-SENSOR CONFIGURATIONS AND BOTH THREE AND FOUR SENSORS IN AGREEMENT REQUIRED FOR MULTISITE DETECTION.

Configuration I

Three-at-a-Time Detections

ϵ \ n_{fa}	1	2	3	4
0.25	2.0	10.8	19.6	29.0
0.10	2.1	13.8	28.9	40.0
0.01	2.2	15.9	49.9	78.8

Four-at-a-Time Detections

ϵ \ n_{fa}	1	2	3	4
0.25	0.0	0.8	4.5	4.8
0.10	0.0	0.2	1.7	3.0
0.01	0.0	0.0	0.4	0.2

Configuration II

Three-at-a-Time Detections

ϵ \ n_{fa}	1	2	3	4
0.25	3.1	15.9	36.0	55.4
0.10	3.2	18.9	49.8	86.9
0.01	3.2	22.8	70.8	175.8

Four-at-a-Time Detections

ϵ \ n_{fa}	1	2	3	4
0.25	0.1	1.2	5.8	14.4
0.10	0.0	0.6	3.3	10.7
0.01	0.0	0.1	0.4	2.6

TABLE II

SIMULATION PERFORMANCE SUMMARY FOR SENSOR CONFIGURATION I WITH TWO FALSE ALARMS PER SENSOR AND ONE REAL TARGET. AVERAGE PERFORMANCE OVER TEN TRIALS IS SHOWN AS A FUNCTION OF THE WINDOW PARAMETER, ϵ, AND THE STANDARD DEVIATION, σ, OF RANGE MEASUREMENTS. (a) THREE-AT-A-TIME DETECTION REQUIRED. (b) FOUR-AT-A-TIME DETECTION REQUIRED.

	σ								
	0.0			0.01			0.05		
	ϵ			ϵ			ϵ		
	0.25	0.1	0.01	0.25	0.1	0.01	0.25	0.1	0.01
Number of Possible Targets	22.4	34.5	57.9	22.6	34.3	58.3	22.1	33.8	56.4
Redundancy of True Target	21.4	16.0	10.4	21.2	15.5	7.2	20.4	11.5	5.2
False Targets with Excess Redundancy	0.6	0.3	0.0	0.4	0.3	0.0	0.3	1.5	5.8

(a) Three-at-a-Time Detections

	σ								
	0.0			0.01			0.05		
	ϵ			ϵ			ϵ		
	0.25	0.1	0.01	0.25	0.1	0.01	0.25	0.1	0.01
Number of Possible Targets	3.7	2.8	1.4	3.5	2.6	0.9	4.1	2.9	0.8
Redundancy of True Target	6.6	5.1	4.0	6.5	4.7	0.9	6.4	2.4	0.3
False Targets with Excess Redundancy	0.2	0.0	0.0	0.1	0.1	0.3	0.1	0.5	0.3

(b) Four-at-a-Time Detections

A true target report and two false alarms per sensor is the same total number of reports as three false alarms from each sensor. As we might expect, the total number of possible targets produced by our multisite detection algorithm is similar for the two cases. This can be seen by comparing the three-false-alarm column of the Configuration I side of Table I with the "number of possible targets" entries in Table II.

In Table II, the "redundancy of true target" entries indicate the number of targets which the multisite detection algorithm put into the cluster which corresponded to the true target position. The "false targets with excess redundancy" entries are the average number of other clusters with at least as many members as the cluster corresponding to true target. In interpreting these data, it is helpful to know the target redundancy which our multisite detection algorithm would produce for the case of no single-site false alarms, perfect range reports, and infinite precision arithmetic. The values are ten for the three-at-a-time detection case and four for the four-at-a-time detection case.

We see from Table II that true target redundancy is at least as large as the baseline values of ten and four if the window parameter, ϵ, is large relative to the standard deviation, σ, of range measurement errors. When ϵ is reduced to be of the order of σ, the true target redundancy starts to become depressed with an increasing probability of actually missing a target. If ϵ is reduced much more, the probability of missing a true target is substantially increased. This is clear for the case of four-at-a-time detections with $\epsilon = 0.01$, $\sigma = 0.05$. In that case, the average redundancy of the true target is 0.3 indicating that a large fraction of the time no cluster was obtained which could reasonably correspond to the true target position.

As ϵ is reduced below σ with a corresponding decrease in the redundancy of true targets, the number of false targets with excess redundancy also increases. This is quite clear in the three-at-a-time case with $\epsilon = 0.01$, $\sigma = 0.05$. It is less clear for four at a time since the number of false alarms is small even for the case of no targets and three single-sensor false alarms per sensor (see Table I).

Finally, the data in Table III are less detailed but similar to those in Table II. The main difference is that Table III presents data for two targets and a single false range report

TABLE III

SIMULATED PERFORMANCE SUMMARY FOR SENSOR CONFIGURATION I WITH ONE FALSE ALARM PER SENSOR AND TWO REAL TARGETS. AVERAGE PERFORMANCE OVER TEN TRIALS IS SHOWN AS A FUNCTION OF WINDOW PARAMETER, ϵ, AND THE STANDARD DEVIATION, σ, OF RANGE MEASUREMENTS. ALL DATA ARE FOR THE MINIMUM CASE OF THREE CONSISTENT RANGE REPORTS REQUIRED FOR MULTISITE DETECTION.

	σ								
	0.0			0.01			0.05		
	ϵ			ϵ			ϵ		
	0.25	0.1	0.01	0.25	0.1	0.01	0.25	0.1	0.01
Number of Possible Targets	23.2	33.3	72.4	23.6	33.8	73.9	24.4	34.3	71.0
False Targets with Excess Redundancy	0.7	1.7	0.1	1.2	2.1	0.7	1.3	1.9	*

generated by each sensor site. In all cases except the starred entry, a cluster was generated for both of the actual targets for every run. In the case of the starred entry, several of the ten runs failed to generate a cluster for one or both of the true targets. The false target entries in the table correspond to the number of non-target clusters with at least as many members as either of the two true target clusters. Although there are some false targets, these results and those discussed earlier suggest that multisite detection will be a difficult but not impossible task and that it can be greatly aided by the proper use of redundant data.

3. Revised Approach to Multisite Detection

Our existing simulation of a range-only system contains a critical inner routine which operates on three simultaneous range measurements to generate a target location or declare no target if the ranges are inconsistent. Target reconstruction (multisite detection) is by synthesis from the sensor data. This is acceptable for a simple range-only system with simultaneous reports from several sensors. However, if reports are not simultaneous or other target measurements (range rate, acoustic azimuth, apparent acoustic frequency) are involved, it becomes necessary to develop a target synthesis algorithm for every combination of report times and data types. One could choose only to declare multisite targets for a small set of possible kinds of sensor reports. This would unfortunately exlude the possibility of tracking targets which the system should in fact be able to handle. A more general and adaptable approach to multisite detection has been identified and is briefly described below.

The new approach to multisite detection is informally characterized by the following discussion which considers constant-velocity targets for simplicity. At any instant in time, the geographic and velocity space in which targets exist can be quantized into cells. For each cell, the actual sensor data over some time window can be compared with data predicted for a target in that cell. Cells which cause enough data to match can be declared to contain targets. A distinct advantage of this approach is that we need only be able to calculate what a sensor should report given a target state and need not invent a new synthesis algorithm for each situation. The revised approach is a search through target state space while doing hypothesis testing at each step along the way. It allows many options for searching, data matching, and decision algorithms. They can be ad hoc, heuristic, or derived from theoretical models. It will allow for almost any kind of information to be used in the process.

It should be noted that the combinatorial and computational characteristics of the revised approach and the approach represented by the software discussed in previous sections are quite different. Suppose that a multisite detection processor is dealing with M sensors and that each sensor is reporting K ranges for possible targets. The straightforward synthesis approach represented by the programs we have already written could require up to $M!K^N/[(M-N)!N!]$ combinations of N sensor reports to be checked in order to produce its list of candidate targets. Undoubtedly the problem could be mitigated by using modern software techniques to avoid exhaustive searching. However, the point to note is that the computational load will tend to grow very quickly as the number of sensor reports and the number of sensors increases. The analysis approach will have its own but different related computational problems. For this approach, the load appears to grow only linearly with the number of sensors and number of sensor reports. However, in principle a search of the entire target state space will be required at every instant in time. Methods for avoiding this without missing excessive numbers of targets will be required.

11

D. Sensitivity Analysis

Multilateration is the standard radar term for locating targets by means of multiple range reports. If it is used, which is not very often, the usual objective is to obtain better target locations. Multisite detection is not traditionally an issue since the individual radars can replace that function. Work on multilateration usually focuses upon the shape and size of target location error ellipsoids as a function of the geometrical relationship between targets and sensors and the errors of observation. Some results of interest to the DSN are well known. One is that for ground-based radars and airborne targets a most desirable geometry is one where the lines from target to radars all lie roughly on a 90-deg. cone. Another is that height accuracy of a system in which a target is at a low elevation angle for all radars can be much improved by a single radar for which there is a much larger elevation angle. Work of this kind has been reviewed with an eye towards doing the same thing for different kinds of sensor reports and for mixes of different kinds. A related issue is the impact of sensor location errors upon the accuracy of target locations. We have formulated the basic equations which can be transformed into computer programs to study sensitivity issues related to multisite detection and to sensor mixes in a DSN. Knowledge of sensitivity will be required not only to evaluate location quality but also to support the development of multisite detection algorithms.

Our sensitivity analysis is based upon weighted least squares estimation and the following general model. Let p be a vector of unknown parameters to be estimated. Most typically its components will be the location and perhaps the velocity of a target of interest. Let q be a second parameter vector whose components are assumed known but that there may be errors in the assumed values. One example of a q vector might be a vector containing the coordinates of all sensors being used to locate a target. The observations available for locating targets are, in the absence of noise of any kind, assumed to be functions of p and q. These noise-free observations are $x_i(p,q)$, $i = 1,\ldots N$ which can be arranged as a vector $x = \text{col}(x_1 \ldots x_N)$. The components could, for example, be sensor-to-target ranges or range rates for simple monostatic radars. In practice, the x_i cannot be directly observed and we assume additive noise to give the noisy observations $y_i = x_i + w_i$ where the w_i are the additive noise. In vector notation $y = x + w$. The noise vector w is assumed to have mean value zero and covariance matrix $W_o = Eww^T$ where E stands for expected value and T denotes transposition.

One method which can be used to estimate p is to minimize the quadratic loss function

$$J^2(p) = [y - x(p)]^T \, W^{-1} \, [y - x(p)]$$

where the dependence on q has been notationally suppressed and W^{-1} is a weighting matrix.

For an estimate of the above type, we can relate errors in the estimate of p to the observation errors, w, and to the errors in our knowledge of the q parameter vector. This can be done by linearizing around the true values p_0, q_0 and obtaining an expression for the covariance matrix of the errors in the p estimate. Let R be that covariance matrix. It is given by

$$R = (P^T W^{-1} P)^{-1} (P^T W^{-1} W_0 W^{-1} P) (P^T W^{-1} P)^{-1}$$

$$+ (P^T W^{-1} P)^{-1} (P^T W^{-1} Q B Q^T W^{-1} P) (P^T W^{-1} P)^{-1}$$

Where P, Q are gradient matrices with elements P_{ij} and Q_{ij} which are the derivatives of x_i with respect to p_j and q_j, respectively, and evaluated at p_0, q_0 and B is the covariance matrix of

possible errors in the assumed values of q_0. In obtaining this, we assume the observation errors and errors in q are independent and zero mean. In this case, the parameter estimate errors are also zero mean and, moreover, if observation and q errors are normally distributed, then so are the estimate errors. The expression for R simplifies considerably if $W_0 = W$.

The error moment matrix, R, is a complete characterization of target location errors given the assumptions of our model. According to our assumptions, the error vector, α, is normal and, for C a constant, $C^2 = \alpha^T R^{-1} \alpha$ defines an ellipsoid on which the probability density of α is constant. The shape and volume of such ellipsoids as a function of sensor types and system geometry will be the object of continuing work. The character of those ellipsoids will be easily studied through the eigenvalues and eigenvectors of R^{-1}.

III. SENSOR INVESTIGATION

Thus far, our detailed sensor investigations have focused exclusively upon acoustic and seismic sensors. The goal has been to establish the utility of acoustic/seismic signals from moving vehicles for detection, location, classification, and tracking in a multiple-target environment. Once acoustic parameters have been determined, acoustic-only and combined acoustic-radar system trade-offs may be quantified and applied to the preliminary design of a test-bed system. The impetus for investigating acoustics lies in the fact that most vehicles, be they land, air, or seagoing, are powerful sound emitters and that microphones are inexpensive, easily deployable, passive, and not especially vulnerable to countermeasures. We note that our particular interests cover a wide variety of acoustic phenomena, including underwater acoustics, seismic and seismo-acoustics, and atmospheric acoustics associated with low-flying targets.

Our efforts to date cover the following: (1) prediction of acoustic and seismo-acoustic propagation phenomena with respect to normal variations of the atmosphere, and (2) design and implementation of an experiment that will show the actual capabilities and feasibility of an acoustic-only or an acoustic-aided distributed sensor network for the surveillance of multiple low-flying targets.

A. Acoustic/Seismic Field Experiment

During June 1977, a field operation was conducted at Fort Huachuca, Arizona, for the purpose of collecting acoustic and seismic array data for low-flying aircraft traveling at subsonic velocities. This experiment differed from all previous work known to us in that the position of the aircraft as a function of time was obtained by recording radar tracking information on digital tape.

The radar tracking and recording service was provided by the United States Army Electronic Proving Ground (USAEPG), Fort Huachuca, Arizona. In addition, USAEPG arranged for aircraft, communication facilities, power, balloon flights to gather meteorological data, surveillance radar, and general physical support. The acoustic and seismic measurement and recording equipment and the necessary personnel to set up and operate it were provided by the United States Army Corps of Engineers Waterways Experiment Station (WES). WES also provided the analog-to-digital data conversion services at their facility in Vicksburg, Mississippi.

In addition to source location requirements, the experiment was designed to include as complete a set of the various aircraft source types as possible and known atmospheric acoustic transmission characteristics. There are essentially four different aircraft acoustic source types, and one of each class was employed in the experiment. The aircraft were: an A-7 jet, a Mohawk OV-1D twin-engined turboprop, a Beechcraft U-8 twin reciprocating-type prop, and a UH-1 Huey helicopter. To adequately cover the possibility of atmospheric propagation problems, the experiment was designed such that each aircraft flew reversed tracks 30 km in length at altitudes of 70 m, 300 m, and 1 km above the recording site, and a circular track of radius 4 to 5 km about the recording site. The tracks were repeated at various times when predicted meteorological conditions might have caused significant differences in acoustic propagation characteristics. To firmly establish acoustic propagation characteristics at those times, two meteorological balloon flights were conducted at the expected extreme acoustic conditions, early morning and mid-afternoon. The aircraft flight paths were radar tracked and controlled and recorded on digital tape. Synchronized acoustic data were analog recorded at the sensor site.
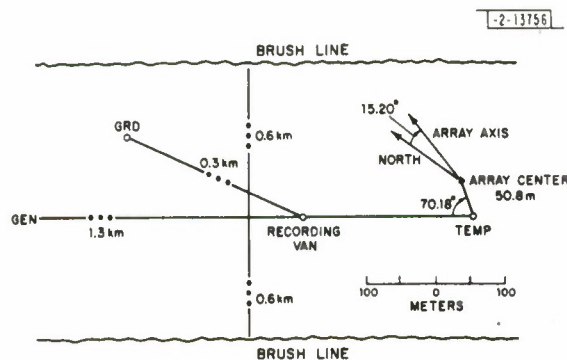
Fig. III-1. Acoustic-seismic sensor
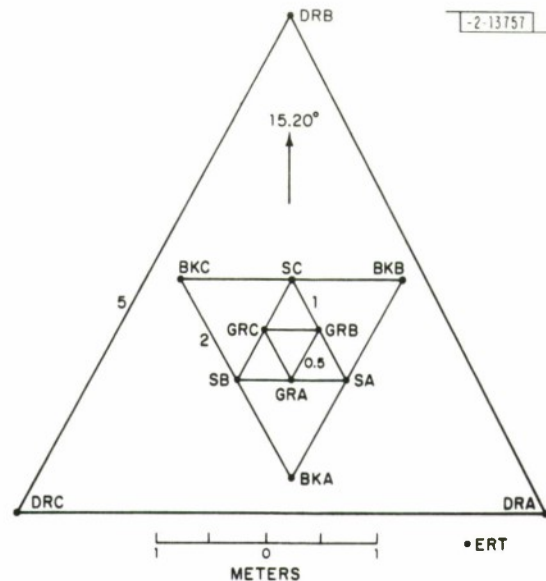and recording van setup.

Fig. III-2. Acoustic-seismic
array setup.

The acoustic-seismic sensors and recording van setup is shown in Fig. III-1, and the array setup is shown in Fig. III-2. The array was designed to provide unaliased yet complete and resolvable wavenumber coverage appropriate to the frequency range 5 to 300 Hz for phase velocities of the speed of sound and greater. Referring to Fig. III-2, the instruments beginning with GR were General Radio type 1560-P5 microphones, BK were B & K type 4165 microphones, DR were CBS type 6065 three-component gradient microphones, ERT was a General Radio type 1961-9601 electret microphone, and S were three-component Mark Products L-4 geophones. The seismometers were placed approximately 15 cm below ground level on cement piers. ERT was placed at 3 m above ground level, and all of the other microphones at 1 m above ground level. A GR microphone was placed approximately 1/2 km NW of the array to obtain large range signal coherence information.

During field operations, approximately 15 hours of aircraft acoustic and seismic data were recorded on analog tape. An additional amount of time was spent recording ambient noise conditions during various parts of the day and night and conducting instrument calibrations. To date, 100 5-sec intervals of the data representing each aircraft type have been digitized at 5000 Hz. Figures III-3 through -6 show examples of digitized data for each aircraft type on various instruments. We note that, as expected, blade-rate harmonic-type signals dominate for prop-driven aircraft and that overall signal coherence is high for all aircraft types. We also observe good S/N ratios in the data. The OV-1D data were taken during extremely bad surface wind conditions (gusting to 25 knots). However, the acoustic noise from the wind is well out of the signal band and the inband S/N is still quite high. Note that acoustic signal detection characteristics are not necessarily severely affected by high ambient noise fields if the data have sufficient dynamic range and signal and noise have different spectral or spacial characteristics. More detailed studies of detection range, classification, tracking, and location are addressed in the following sections.
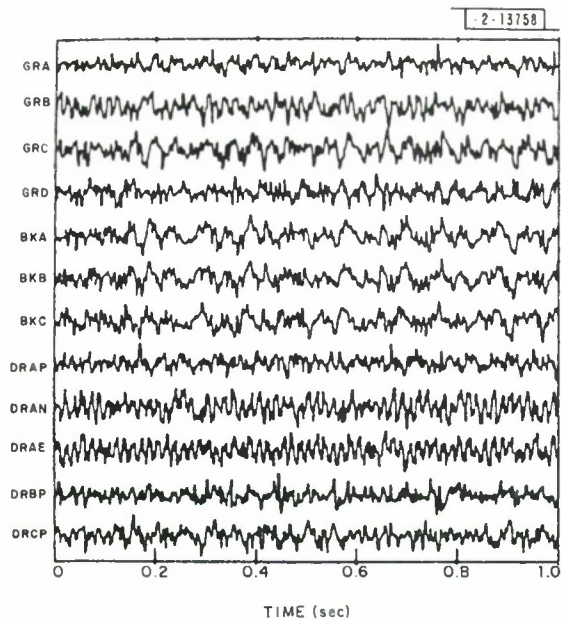
Fig. III-3. Segment of U-8 acoustic digital data at an acoustic range of 5 km inbound.
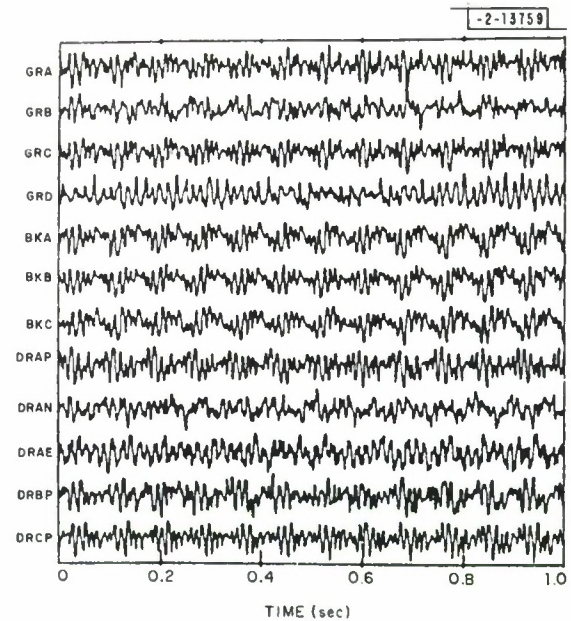
Fig. III-4. Segment of UH-1 acoustic digital data at an acoustic range of 8 km inbound.
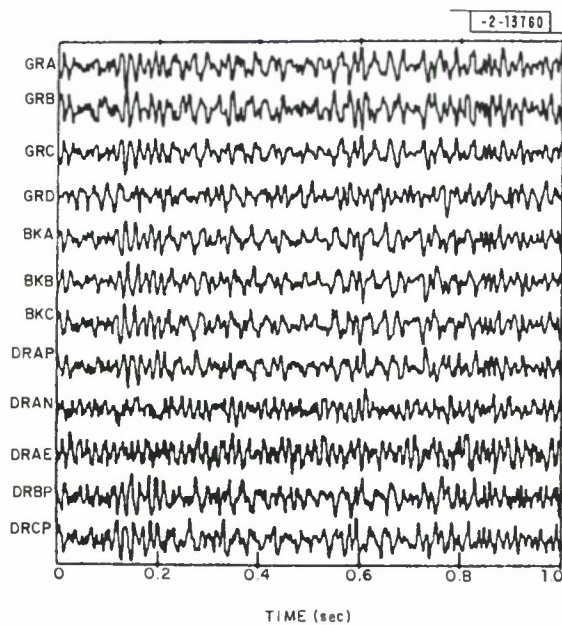
Fig. III-5. Segment of A-7 acoustic digital data at an acoustic range of 8 km inbound.
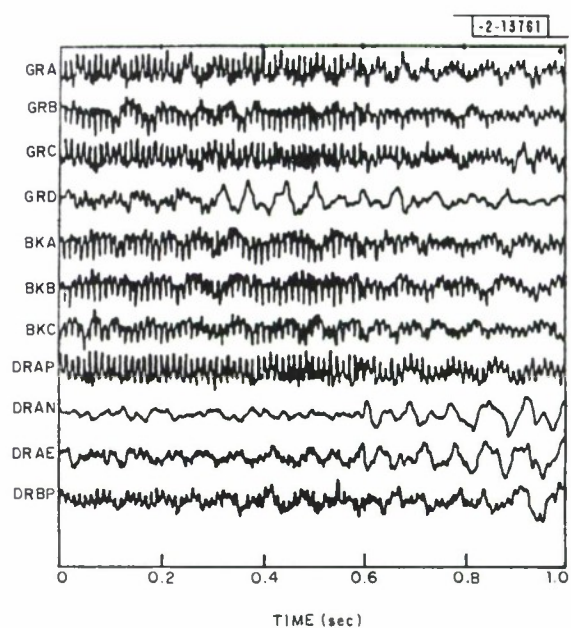
Fig. III-6. Segment of OV-1D acoustic digital data at an acoustic range of 1.2 km inbound under severe surface wind conditions.

B. Analysis and Evaluation of Experimental Data

Preliminary results based on a review and analysis of a part of the experimental data are summarized in the following sections. In order to interpret the results properly and to understand the use of acoustic sensors in a DSN, one must be aware of certain significant moving-source and atmospheric-propagation effects. These effects are reviewed in the sections preceding the analysis and evaluation.

1. Moving-Source Effects

Consider that at time t a sound source, moving at constant velocity v, is at a distance vt from the closest point of approach (cpa) to an observation point O. Let the distance between O and cpa be r so that the distance of the source from O at time t is

$$D(t) = \sqrt{r^2 + v^2 t^2} \quad .$$

The sound arriving at O came from the source when it was at some earlier position, say a distance of R from O. The time required for sound to travel R (i.e., R/c, where c equals

Fig. III-7. Geometry for the analysis of kinematic parameters for a constant-velocity source.
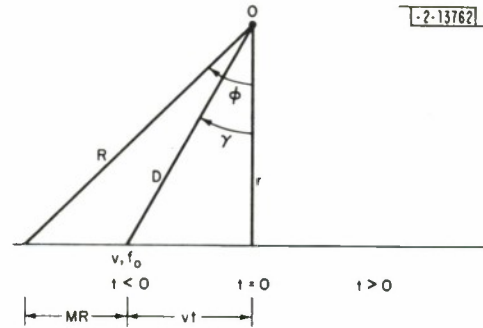
the speed of sound) will equal the time the source took to move from R to D. Let that be a distance L. Since the source moves at v, then we have L/v = R/c so that L = MR where M, the Mach number, is defined as v/c. The geometry of this situation is shown in Fig. III-7. From the figure we have

$$R^2 = r^2 + (MR - vt)^2$$

and so, for subsonic v, the acoustic range is given by

$$R(t) = [-Mvt + \sqrt{(1 - M^2)r^2 + v^2 t^2}]/(1 - M^2) \quad .$$

Using this relationship, the following relationships are found[*]: the true azimuth,

$$\gamma(t) = \tan^{-1}(-vt/r) \quad ,$$

the acoustic azimuth,

$$\varphi(t) = \tan^{-1}[(MR - vt)/r] \quad ,$$

the perceived frequency when the source is emitting a frequency f_o,

$$f(t) = f_o/[1 - M \sin(\varphi)] \quad ,$$

---

[*] P. M. Morse and K. U. Ingard, Theoretical Acoustics (McGraw-Hill, New York, 1968).

18

the acoustic range rate,

$$\dot{R}(t) = -v(f/f_o) \sin(\varphi) \quad ,$$

the acoustic azimuth rate,

$$\dot{\varphi}(t) = -rv(f/f_o)/R^2$$

and the far-field pressure envelope

$$p(t) = (f/f_o)^2/4\pi R \quad .$$

Figures III-8 and -9 show the behavior of these functions for M = 0.75 and M = 0.12, respectively, which are the maximum and minimum values used in the experiment. We note the following properties of these functions which apply to a greater extent for larger Mach numbers and a lesser extent for smaller Mach numbers. As shown in the figures, the acoustic position is delayed relative to the actual position in proportion to the Mach numbers. At large equal distances, the pressure on the incoming path is greater than the pressure on the outbound path by a factor of $(1 + M)^2/(1 - M)^2$. For example, a vehicle traveling half the speed of sound radiates four times the power forward as backward. Additionally, the peak pressure comes before the vehicle is at cpa. Finally, we note that large changes in azimuth, excess pressure, and doppler (f/f_o), take place primarily in the region when the vehicle is within about $\pm r/c$ of cpa.

2. Meteorological Data Analysis

In support of the experiment conducted at Fort Huachuca, two balloons were launched to gather sound speed, wind velocity, and relative humidity data. Flights were scheduled during the expected most extreme acoustic conditions. The purpose was to obtain an appropriate data base for determining the importance of sound refraction and attenuation in observed detection range and signal variation. The first balloon was launched during the mid-afternoon (approximately 1500 local time) when the normal lapse rate would have a high positive temperature gradient approaching the ground surface. During such conditions, the sound velocity profile is monotonically decreasing upwards causing sound energy to be continuously refracted upward at every level of the troposphere. Under such conditions, detection ranges should be less than average. Additionally, small- and large-scale thermal convection should have non-negligible acoustic effects by increasing the background acoustic noise level (wind noise) and introducing asymmetry in propagation characteristics. This phenomenon is due to wind velocity gradients altering the effective sound velocity profile as a function of propagation direction. Figure III-10 shows the meteorological data collected during this time span. The wind direction is not shown although those data were also obtained from the balloon tracking data. The sound speed was derived directly from the temperature data. Figure III-11 shows the east-west geometrical propagation characteristics (based on ray tracing[*]) for sources at 200, 900, and 3000 ft above ground level. Only the critical distances are indicated and not the ray paths. Theory predicts shadow zones at 2.1 km west and 1.8 km east for the source at 200 ft altitude; i.e., all rays that start out more horizontal or upward than the critical rays are turned upward before reaching

---

[*] R. J. Thompson, "Compiling Sound Ray Paths in the Presence of Wind," SC-RR-67-53, Sandia Laboratory, Albuquerque, New Mexico (1967).
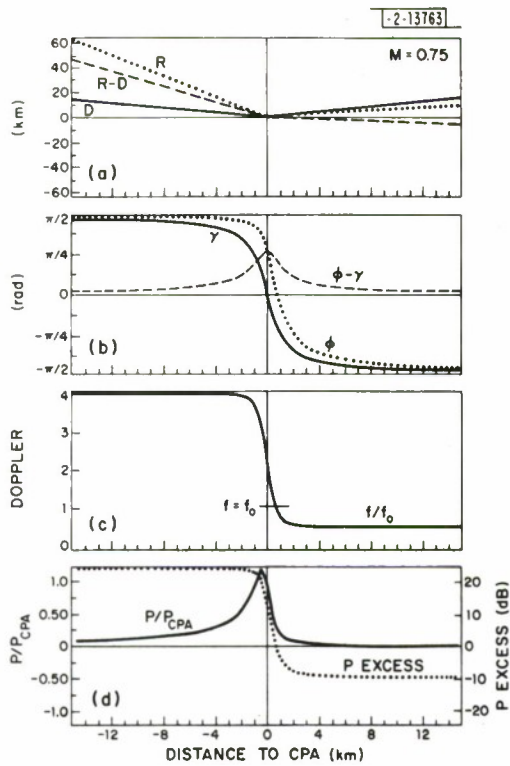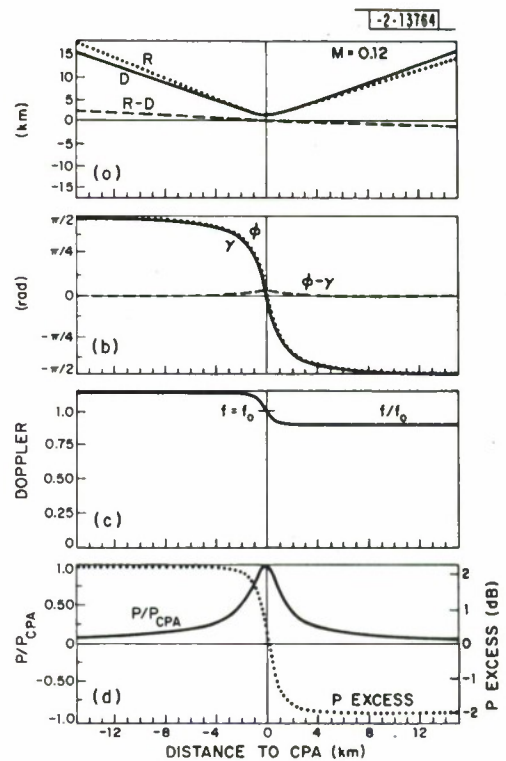
Fig. III-8. Kinematic and dynamic characteristics of sound received from a Mach 0.75 flyby. The characteristics are shown as a function of the aircraft distance from cpa. Negative distance is for the incoming path. (a) Acoustic range R, actual range D, and their difference. (b) Acoustic azimuth φ, actual azimuth γ, and their difference. (c) Doppler f/f_o. (d) Ratio P/P_{cpa} of pressure to pressure at cpa and, P_{EXCESS}, the excess pressure above pressure that would be observed if the source were stationary.

Fig. III-9. Same as Fig. III-8 but for Mach 0.12.

Fig. III-10.   Mid-afternoon
meteorological balloon data.

1,2,3 PRIMARY AIRCRAFT
FLIGHTPATH ALTITUOES

SITE ELEVATION
(4225 ft)

0	12	24	36	T (Temp. °C)
1060	1090	1120	1150	C (Speed of Sound-ft/sec)
	9	15	21	27	W (Wind Speed-ft/sec)
	15	30	45	60	R (Relative Humidity-%)

·2·13766

Fig. III-11.   Primary critical points and their geometrical
shadow zones for afternoon conditions.

21
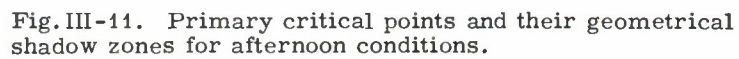
the ground. Similar statements are true for the sources at the higher altitude with the shadow zone distances given in the figure. The theory also predicts that some energy in the field from the source at 900 ft altitude is ducted in an easterly direction. Given changes in the meteorological conditions, or changes in topography, such energy might be detected at large ranges. It is noted that detection range (assumed proportional to the shadow-zone range) is directly proportional to the source altitude for these meteorological conditions.

The second balloon was launched during the early morning (approximately 0300 local time). At this time, the normal lapse rate should be underlain by a high negative temperature gradient approaching the ground surface. Under these conditions, the sound-speed profile has a zone of low values near the surface. Energy entering that zone will be refracted toward the ground, increasing the effective detection range. During periods when such velocity conditions persist, better than average detection ranges should be encountered. Upper level winds during this time period may also have severe propagation path effects. However, there is not much small-scale lower level turbulence and consequently low background noise levels should be encountered. Figure lll-12 shows the balloon data collected during this early morning flight, and Fig. lll-13
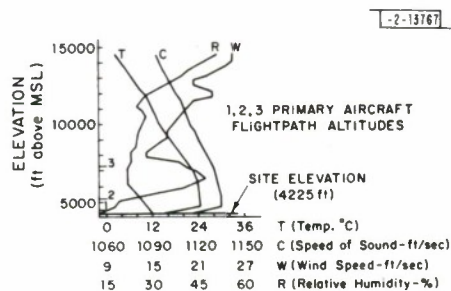
Fig. lll-12. Early morning meteorological balloon data.
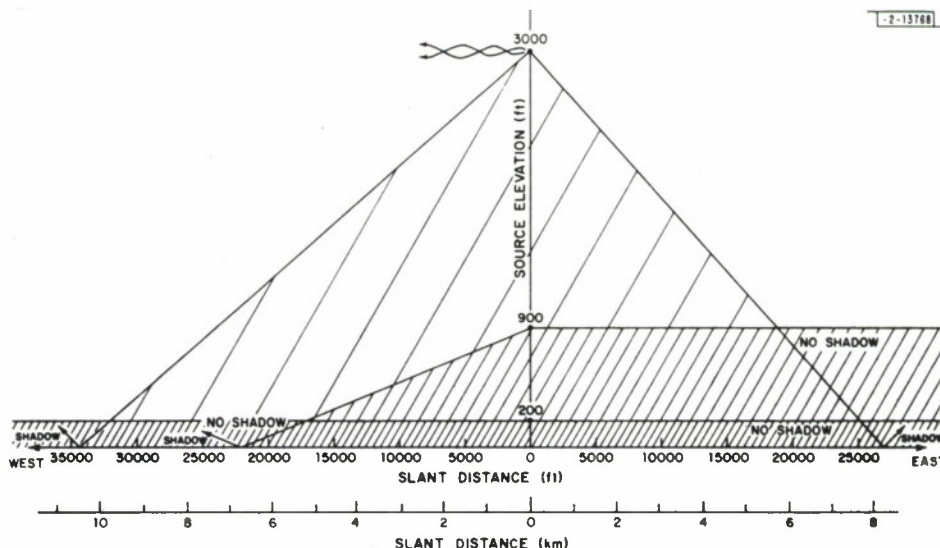
Fig. lll-13. Primary critical points and their geometrical shadow zones for early morning conditions.

shows the ray-tracing results based on these data. Just opposite to the mid-afternoon results, the lowest source has the largest detection range. Again, winds produce asymmetry and some ducting occurs, but overall much larger propagation distances can be expected during these conditions.

In summary of the theoretical ray-tracing results, we expect geometrical detection ranges of at least ±10 km for all low-flying vehicles during good acoustic periods and of at least a few kilometers during unfavorable acoustic conditions. Ambient noise conditions due to surface winds, rain, etc., will of course make detection more difficult but should not significantly change the above effects for systems of sufficient dynamic range. In reality, larger detection ranges should be expected since some energy will be diffracted and possibly scattered into the shadow-zone region. Lastly, when wind gradients are on the order of normal sound-speed gradients, asymmetrical propagation conditions will exist.

3. Observed Detection Ranges

To date, only a small portion of the digital data has been available for analysis; however, direct analog plots of most of the acoustic data were obtained in the field. Unfortunately, the time base on these plots is known only to within a few tens of seconds, or equivalently the aircraft location is known only to within a few kilometers. Additionally, plotter noise starts at about 30 dB below full scale. The result is that when using the plotted analog data, estimated acoustic range may be in error by about a kilometer and maximum signal dynamic range will be about 35 dB. Figures III-14 to -18 show the amplitudes of detected signals on these analog plots as functions of acoustic range. The acoustic range was derived from the radar tracking data and the moving source effect formulas given in Section III-B-1. The solid curved lines on the plots indicate normal geometrical spreading for a homogeneous atmosphere. The vertical lines show the geometrical shadow boundaries determined in the meteorological data section of this report. Finally, the peak noise level is given by the horizontal lines.

The data presented in the figures can be summarized as follows: in all cases, with only 35 dB of effective dynamic range, the aircraft were acoustically detectable out to at least 10 km, although not always on both the inbound and outbound paths. Amplitudes die off at about the geometrical rate, appropriate to a homogeneous atmosphere, up to the calculated geometrical shadow boundary for actual atmospheric conditions. In the diffracted region, signal levels are diminished as expected, though still at detectable levels. These observations, which are consistent with predictions based on measured meteorological conditions, indicate that while theoretical propagation characteristics are important they are not severely limiting. Finally, we note that even though the ambient or background noise level is often considerably greater than the signal level, the detection level is still high since the noise and signal energy are well separated in frequency.

4. Spectral Observations

Figures III-19 through -25 show spectra computed at 1-sec intervals for each aircraft type during selected parts of their flight paths. Figures III-19 to -23 show the UH-1 helicopter beginning at 4 km inbound, 4 km outbound, and circling at a 5-km distance, respectively. The velocity of the aircraft was about 40 m/sec, therefore each segment represents a change in position of 40 m. The basic blade-rate frequency for the UH-1 was 11 Hz. Figures III-22 and -23 show similar spectra for the U-8, and Fig. III-24 and -25 show spectra for the A-7 and OV-1D,
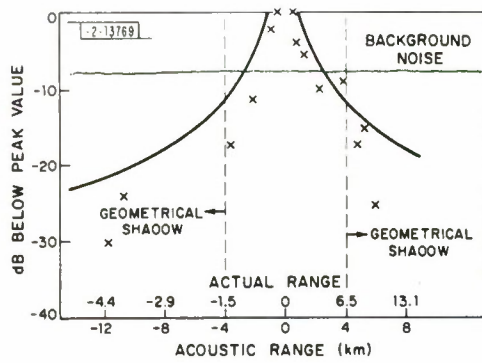
23

Fig. III-14.   Detection data for A-7
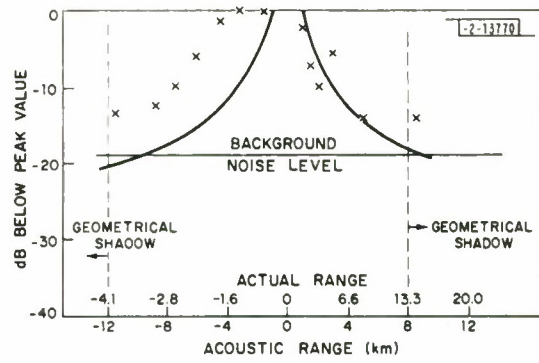(altitude = 450 m, 0 dB = 87 dBa).

Fig. III-15.   Detection data for A-7
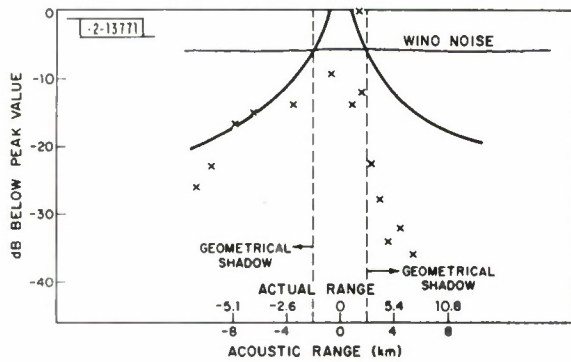(altitude = 1020 m, 0 dB = 62 dBa).

Fig. III-16.   Detection data for OV-1D
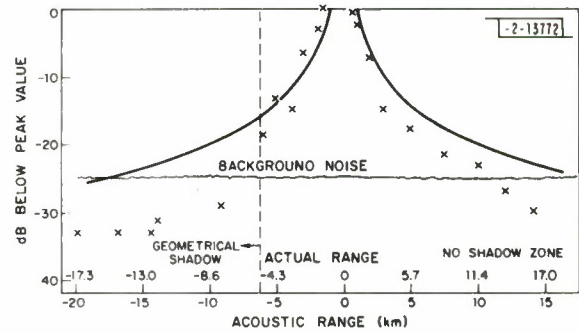(altitude = 75 m, 0 dB = 88 dBa, windy
conditions).

Fig. III-17.   Detection data for UH-1
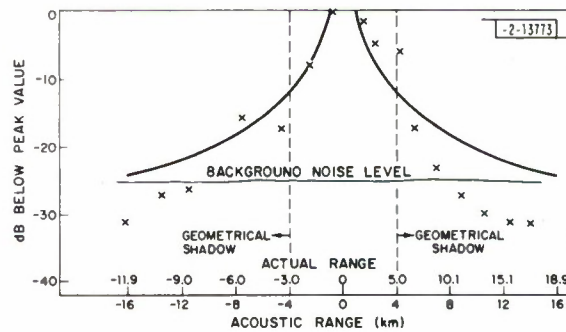(altitude = 300 m, 0 dB = 81 dBa).

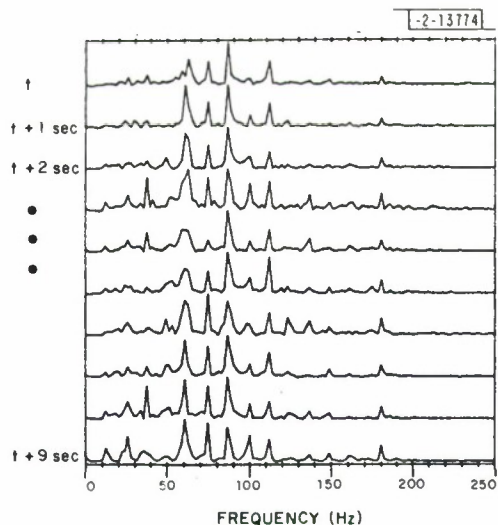Fig. III-18.   Detection data for U-8
(altitude = 300 m, 0 dB = 68 dBa).

24

Fig. III-19. Power spectra on a linear scale for a series of 1-sec (1 sec = 40 m position change) time intervals. Target is a UH-1 inbound with the first spectrum corresponding to a range of 4 km.
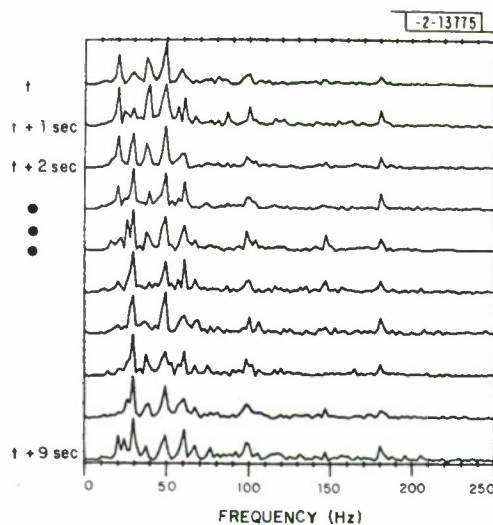

Fig. III-20. Same as Fig. III-19 for the UH-1 at 4 km outbound.
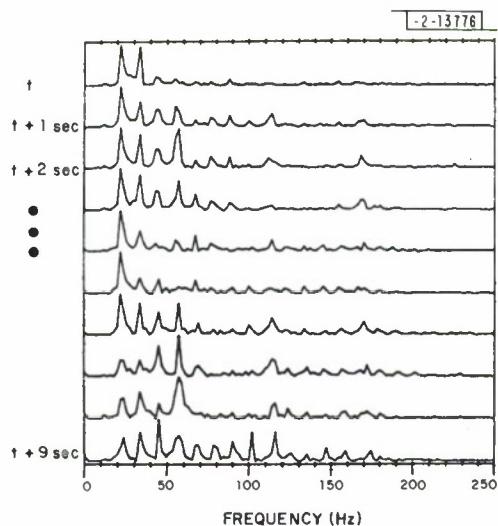
Fig. III-21. Same as Fig. III-19 for the UH-1 circling at 5 km.
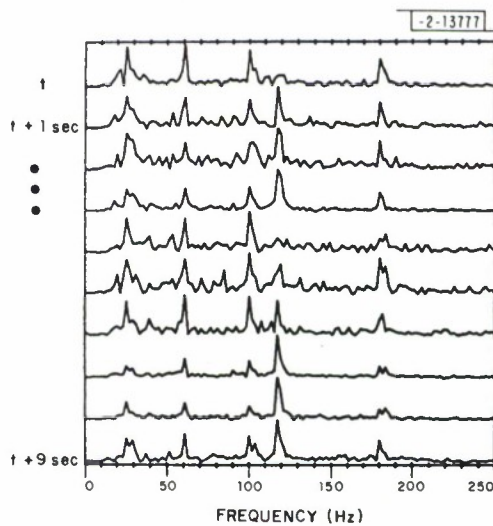
Fig. III-22. Power spectra on a linear scale for a series of 1-sec (1 sec = 80 m position change) time intervals. Target is a U-8 inbound with the first spectrum corresponding to a range of 4 km.

25
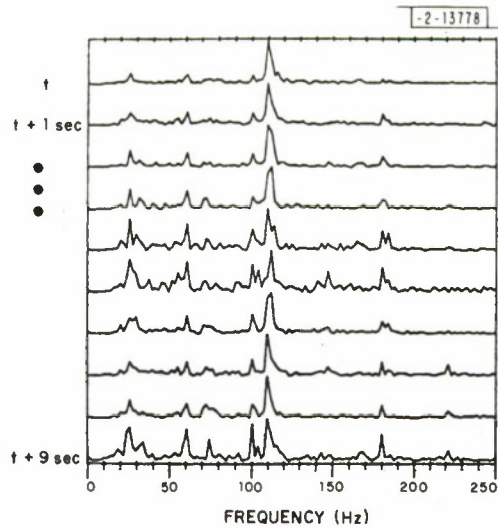
Fig. III-23. Same as Fig. III-22 for the U-8 at 4 km outbound.
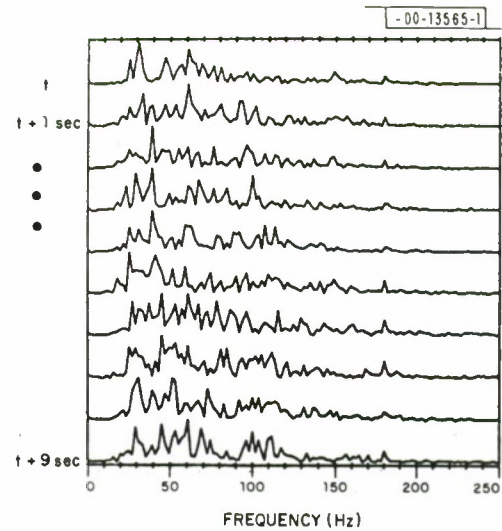
Fig. III-24. Power spectra on a linear scale for a series of 1-sec (1 sec = 210 m position change) time intervals. Target is an A-7 outbound with the first spectrum corresponding to a range of 8 km.
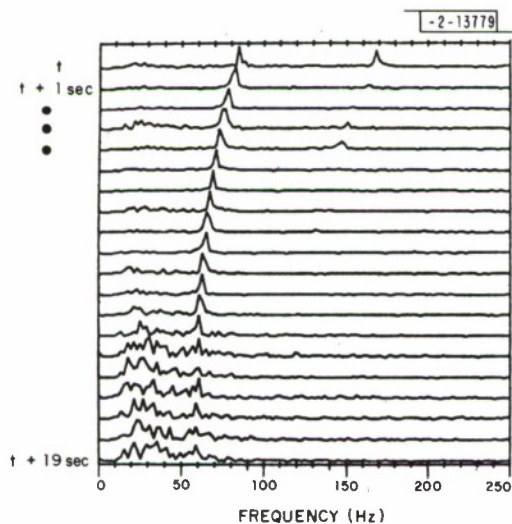
Fig. III-25. Power spectra on a linear scale for a series of 1-sec (1 sec = 110 m position change) time intervals. Target is an OV-1D inbound at an initial range of 1 km.

respectively. Fundamental blade-rate frequency for the U-8 was 180 Hz and shaft rate 60 Hz. The OV-1D blade-rate frequency was 70 Hz. Each spectrum clearly shows that the signal is composed of a combination of fundamental and harmonic frequencies, with the exception of A-7 spectra which have the expected broadband appearance (that would indeed time average to a smooth broadband spectra). We note that the fundamental (or lowest harmonic in the data band) is not necessarily the dominant peak and further, and more important, the overall spectral pattern can be highly dependent on the position of the source with respect to the receivers. In general, such results indicate that target classification (as to jet, turboprop, or helicopter) should be straightforward. However, tracking and multisite target indentification will be more difficult to achieve. As to Fig. III-25, we note the Doppler shift as the OV-1D passes cpa and the low-frequency (but out of the signal band) wind-noise interference during the later portions of the track. Figure III-26 shows the improvement gained with simple high-pass filtering.

5. Array Processing

Conventional and maximum likelihood high-resolution frequency wavenumber array analysis techniques[*] were applied to digital data for the array configuration shown in Fig. III-27. The purpose was to establish the feasibility of making useful azimuth measurements using a small acoustic array. It is important to distinguish between accuracy and precision in acoustics since, while an acoustic wavefront crossing an array may be such that a very precise measurement of its direction and velocity can be made, the direction may not very accurately point to the source from which the sound originated. Inaccuracies of considerable magnitude may be present, due to crosswinds, topographic reflections, horizontal temperature gradients, and, in general, the complicated acoustic nature of the troposphere. Figure III-28 shows the impulse response of the array contoured in 1-dB intervals in wavenumber space. The circle labeled C is the wavenumber corresponding to the speed of sound, and any propagating sound fields crossing the array will have their power within this circle. Figures III-29 and -30 show high-resolution and conventional wavenumber spectra for a UH-1 at 8 km acoustic range. A measure of precision is the width of the 1-dB contour which is a function primarily of the array configuration and chosen frequency. In this case, the width is about 12°. The accuracy is dead on. The conventional spectrum, although less precise, is also dead on in locating the true direction of the source. Figures III-31, -32, and -33 show the results for, respectively, a U-8 at 5 km, an A-7 at 8 km, and an OV-1D at 1.1 km. In each case, the accuracy is well within the precision and on the order of at most a few degrees. While it is premature to judge that acoustic direction will generally be determinable to the accuracy found here, these results indicate that such is possible.

---

[*] J. Capon, Proc. IEEE <u>57</u>, 1408 (1969).
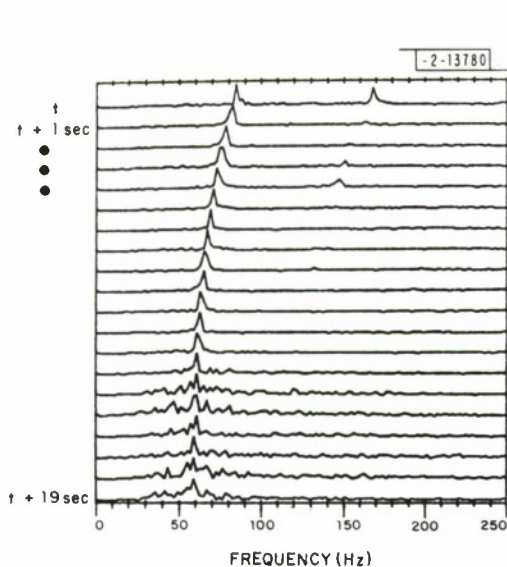
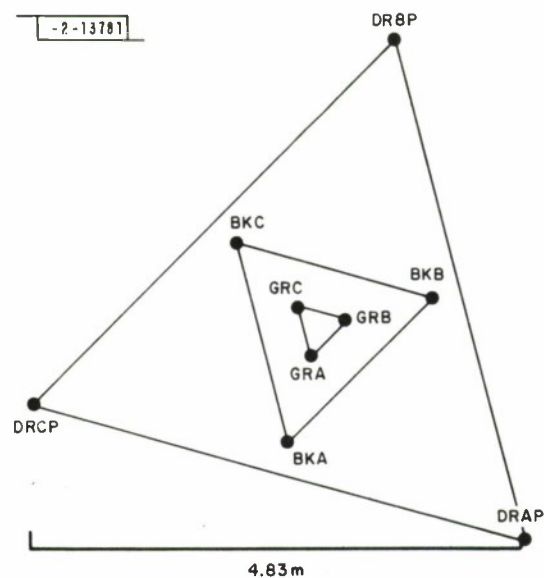Fig. III-26. Same as Fig. III-25 but data preprocessed with a 50-Hz high-pass filter.

Fig. III-27. Sensor stations used for array processing.
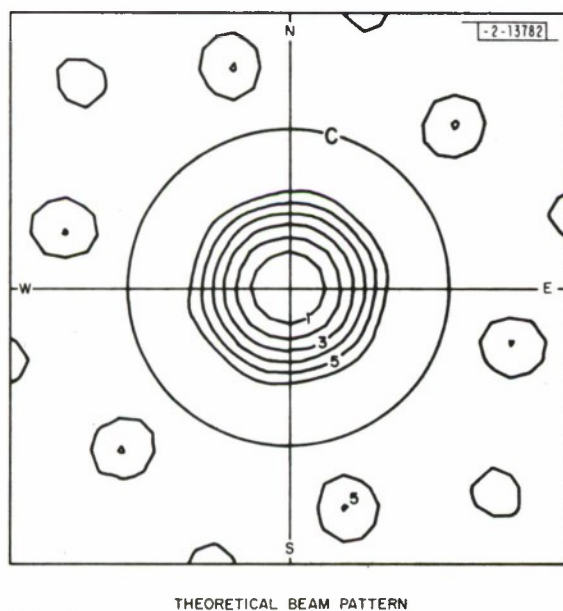

THEORETICAL BEAM PATTERN

Fig. III-28. Wavenumber impulse response of the array of Fig. III-27.
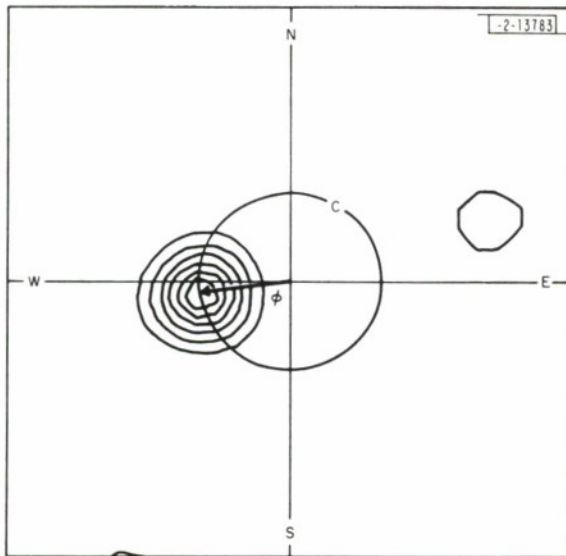
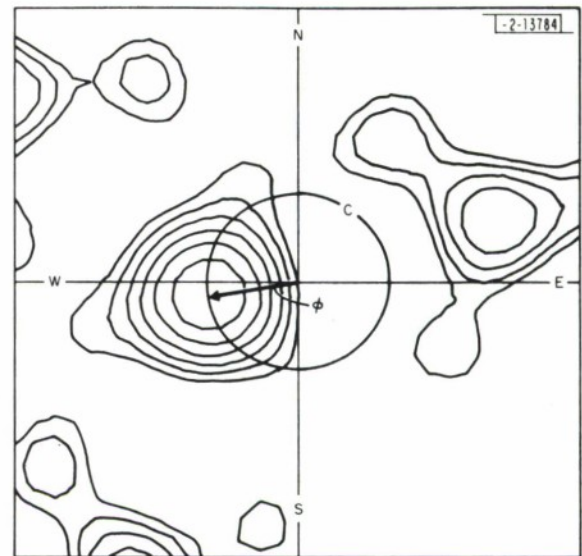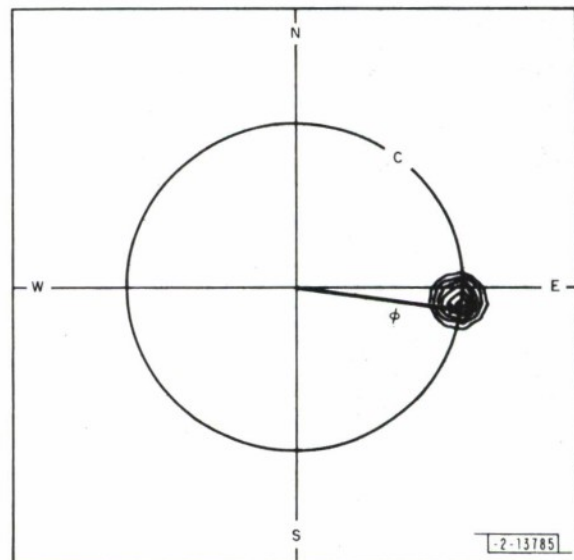Fig. III-29. High-resolution wavenumber spectrum for the UH-1 at 8 km. True azimuth is φ.

Fig. III-30. Conventional wavenumber spectrum of UH-1 at 8 km. True azimuth is φ.

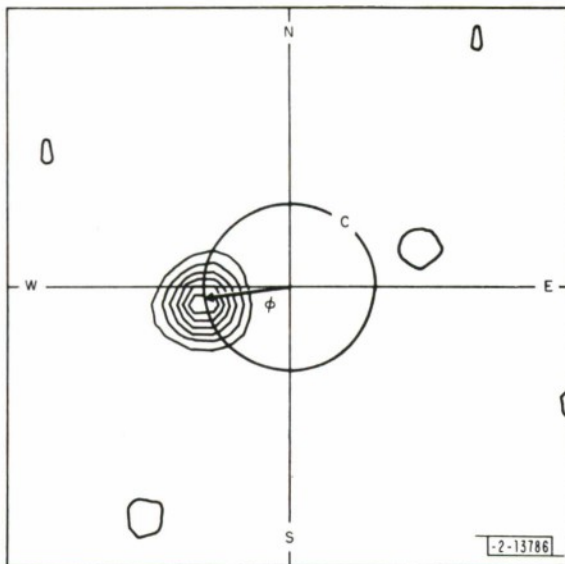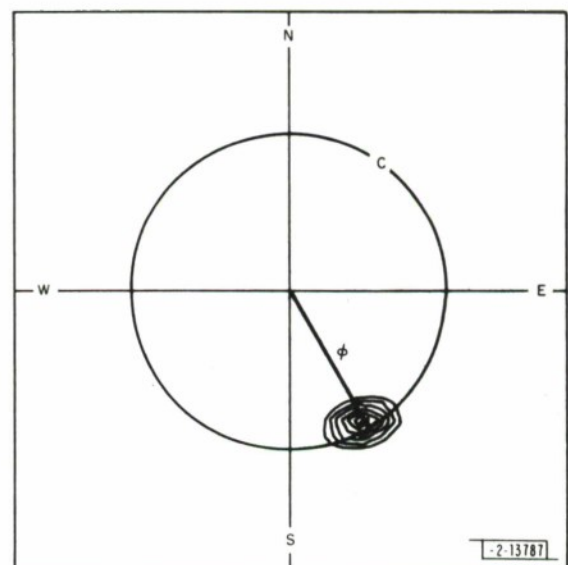Fig. III-31. High-resolution wavenumber spectrum for the U-8 at 5 km. True azimuth is φ.

Fig. III-32.   High-resolution wavenumber spectrum for the A-7 at 8 km.   True azimuth is φ.

Fig. III-33.   High-resolution wavenumber spectrum for the OV-1D at 1.1 km.   True azimuth is φ.

REPORT DOCUMENTATION PAGE		READ INSTRUCTIONS BEFORE COMPLETING FORM
1. REPORT NUMBER ESD-TR-77-279	2. GOVT ACCESSION NO.	3. RECIPIENT'S CATALOG NUMBER
4. TITLE *(and Subtitle)* Distributed Sensor Networks		5. TYPE OF REPORT & PERIOD COVERED Semiannual Technical Summary 1 January – 30 September 1977
		6. PERFORMING ORG. REPORT NUMBER
7. AUTHOR*(s)* Richard T. LaCoss		8. CONTRACT OR GRANT NUMBER*(s)* F19628-76-C-0002
9. PERFORMING ORGANIZATION NAME AND ADDRESS Lincoln Laboratory, M.I.T. P.O. Box 73 Lexington, MA 02173		10. PROGRAM ELEMENT, PROJECT, TASK AREA & WORK UNIT NUMBERS ARPA Order 3345 Project No. 7D30
11. CONTROLLING OFFICE NAME AND ADDRESS Defense Advanced Research Projects Agency 1400 Wilson Boulevard Arlington, VA 22209		12. REPORT DATE 30 September 1977
		13. NUMBER OF PAGES 40
14. MONITORING AGENCY NAME & ADDRESS *(if different from Controlling Office)* Electronic Systems Division Hanscom AFB Bedford, MA 01731		15. SECURITY CLASS. *(of this report)* Unclassified
		15a. DECLASSIFICATION DOWNGRADING SCHEDULE

16. DISTRIBUTION STATEMENT *(of this Report)*

Approved for public release; distribution unlimited.

17. DISTRIBUTION STATEMENT *(of the abstract entered in Block 20, if different from Report)*

18. SUPPLEMENTARY NOTES

None

19. KEY WORDS *(Continue on reverse side if necessary and identify by block number)*

computer network theory
networking
multisite detection
target surveillance and tracking

acoustic, seismic, radar sensors
low-flying aircraft
atmospheric propagation characteristics

20. ABSTRACT *(Continue on reverse side if necessary and identify by block number)*

Progress on the selection of a Distributed Sensor Networks program application problem, discussion of system elements, formulation and testing of multisite detection and location algorithms, and review of the fundamentals of sensitivity analysis are reported. Design and execution of an acoustic/seismic field experiment, and analysis and evaluation of experimental data including preliminary determination of acoustic detection ranges, spectral signatures, and direction determination capabilities are also described.

DD ₁ ᴶᴬᴺ ₇₃ FORM 1473   EDITION OF 1 NOV 6S IS OBSOLETE